



Published in final edited form as:

Arterioscler Thromb Vasc Biol. 2008 April ; 28(4): 685–691. doi:10.1161/ATVBAHA.107.157685.

Dietary cholesterol worsens adipose tissue macrophage accumulation and atherosclerosis in obese LDL receptor-deficient mice

Savitha Subramanian, M.D., Chang Yeop Han, Ph.D., Tsuyoshi Chiba, Ph.D., Timothy S. McMillen, Ph.D., Shari A. Wang, B.S., Antonio Haw III, B.S., Elizabeth A. Kirk, Ph.D., Kevin D. O'Brien, M.D., and Alan Chait, M.D.

From the Departments of Medicine (S.S., C.Y.H., T.C., T.S.M., S.A.W., A.H., K.D.O., A.C.) and Pathobiology (E.A.K.), University of Washington, Seattle, WA.

Abstract

Objective—Chronic systemic inflammation accompanies obesity and predicts development of cardiovascular disease. Dietary cholesterol has been shown to increase inflammation and atherosclerosis in LDL receptor-deficient (LDLR^{-/-}) mice. This study was undertaken to determine whether dietary cholesterol and obesity have additive effects on inflammation and atherosclerosis.

Methods and Results—LDLR^{-/-} mice were fed chow, high fat, high carbohydrate (diabetogenic) diet without (DD) or with added cholesterol (DDC) for 24 weeks. Effects on adipose tissue, inflammatory markers and atherosclerosis were studied. Despite similar weight gain between DD and DDC groups, addition of dietary cholesterol increased insulin resistance relative to DD. Adipocyte hypertrophy, macrophage accumulation and local inflammation were observed in intra-abdominal adipose tissue in DD and DDC, but were significantly higher in the DDC group. Circulating levels of the inflammatory protein serum amyloid A (SAA) were 4.4-fold higher in DD animals and 15-fold higher in DDC animals than controls, suggesting chronic systemic inflammation. Hepatic SAA mRNA levels were similarly elevated. Atherosclerosis was increased in the DD-fed animals and further increased in the DDC group.

Conclusions—Obesity-induced macrophage accumulation in adipose tissue is exacerbated by dietary cholesterol. These local inflammatory changes in adipose tissue are associated with insulin resistance, systemic inflammation and increased atherosclerosis in this mouse model.

Keywords

atherosclerosis; inflammation; obesity; lipoproteins; diet

Chronic systemic inflammation, evidenced as modest, low-grade increases in circulating levels of the inflammatory molecules C-reactive protein (CRP) and serum amyloid A (SAA), is a key feature of the obese state^{1–3}, particularly in visceral obesity^{4, 5}. Adipocyte hypertrophy accompanying obesity is associated with macrophage accumulation in adipose tissue in human subjects^{6, 7}. These macrophages produce cytokines, which cause insulin resistance and signal the liver to produce inflammatory molecules such as CRP and SAA as part of a chronic inflammatory response⁸. Similar changes occur in obese mice^{6, 9}, a species in which SAA functions as the main inflammatory molecule, since CRP levels are not regulated by inflammation¹⁰.

While dietary cholesterol has long been thought to increase atherosclerosis risk in humans¹¹, the mechanism by which this occurs is unclear. Plasma cholesterol levels only increase slightly in response to cholesterol feeding in humans¹², compared to levels occurring in several animal species^{13–15}. Therefore, dietary cholesterol has been postulated to have a lipid-independent effect on atherosclerosis and cardiovascular disease¹⁶. We previously demonstrated that the addition of a small amount (0.15%) of dietary cholesterol to a Western diet resulted in increased circulating SAA and increased atherosclerosis in LDL receptor-deficient mice (LDLR^{-/-}), independent of an effect on plasma lipids and lipoproteins¹⁷. Since increased SAA levels signify a chronic inflammatory state in mice, these findings suggested that inflammation induced by dietary cholesterol might contribute to atherogenesis in this mouse model.

The present study was undertaken to determine whether dietary cholesterol has an additive role in inducing inflammation, insulin resistance and atherosclerosis in the setting of diet-induced obesity. To this end, we chose to induce obesity by feeding a diabetogenic diet rich in saturated fat and refined carbohydrate. This diet has previously been shown to cause obesity, hyperglycemia and increased atherosclerosis in LDLR^{-/-} mice¹⁸. This strain is particularly susceptible to obesity-associated changes induced by the diabetogenic diet, since similar changes were not observed in apo E-deficient mice fed this diet¹⁹. We added 0.15% cholesterol to the diabetogenic diet as in our previous study of LDLR^{-/-} mice¹⁷.

Our observations indicate that the addition of cholesterol to a diabetogenic diet leads to a striking increase in macrophage accumulation in intra-abdominal adipose tissue, evidence of increased insulin resistance and chronic systemic inflammation, and increased atherosclerosis in this mouse model.

METHODS

Animals and diet

Eight week old male LDLR^{-/-} mice bred onto a C57BL/6 background were placed on one of three diets for 24 weeks: a diabetogenic diet high in fat and carbohydrate (DD; BioServ No.F1850, Frenchtown, NJ); diabetogenic diet with 0.15% w/w total cholesterol (DDC; BioServ No.F4997) or standard rodent chow diet (Ch) providing 4% calories as fat. The diabetogenic diet provides 35.5% calories as fat and 36.6% as carbohydrate (Supplemental Table I). Animals were housed in cages with microisolator filter tops, maintained on a 12-hour light/dark cycle in a temperature-controlled room and given free access to food and water. At sacrifice, harvested tissues were snap-frozen at -70°C and/or fixed with 10% neutral-buffered formalin and embedded in paraffin wax. All experimental procedures were undertaken with approval from the Institutional Animal Care and Use Committee of the University of Washington.

Analytical procedures

After 24 weeks of diet-feeding, mice were fasted for 4 h before drawing blood on the day of sacrifice. Plasma insulin was assayed using a commercially available kit (Linco Research Inc., St. Charles, MO). Triglycerides and cholesterol were assayed in plasma and fast-phase liquid chromatography (FPLC) fractions using colorimetric assay kits. Levels of lipoproteins were analyzed by FPLC as described previously. Circulating SAA levels were measured by enzyme-linked immunosorbent assay (ELISA) in plasma and in FPLC fractions from individual mice, as described previously¹⁷. This assay measures SAA isoforms 1 and 2, derived from the liver. Insulin sensitivity was assessed using the homeostasis model assessment of insulin resistance (HOMA-IR), calculated using the formula, blood glucose (mmol/L) x insulin concentration (mIU/L) / 22.5²⁰. Glucose tolerance testing was performed after a 4h fast by intraperitoneal injection of 20% glucose (1.5 mg/g body weight); blood was drawn from the retro-orbital

plexus at 0, 30, 60, and 120 minutes for blood glucose measurements using a glucometer (One Touch Ultra, Lifescan Inc., CA).

Immunohistochemistry

Single-label immunohistochemistry was performed on adipose tissues and aortic sinuses using procedures described previously in detail²¹. Macrophages were detected using a rat monoclonal antibody against Mac2 (titer 1:2500, Cedarlane Laboratories, Ontario, Canada). SAA was detected using a rabbit polyclonal antiserum raised against recombinant human SAA1 (titer 1:500, kind gift of Dr. Frederick de Beer, University of Kentucky, Lexington, KY). Nova Red (Vector Laboratories, Burlingame, CA) was used as the peroxidase substrate to yield a red-brown reaction product; cell nuclei were identified by counterstaining with hematoxylin. Area quantification for Mac2 and SAA was performed on digital images of immunostained tissues using image analysis software (Image Pro; Media Cybernetics, Silver Springs, MD). Area quantification for proteoglycans was performed on digital images of tissues stained with Movat's histochemical stain (collagen stains yellow, elastin stains black, proteoglycans stain blue, fibrin stains bright red, cells stain light red). Two sections per mouse were analyzed. Adipocyte cross-sectional area was measured by computer image analysis using a modification of techniques described previously²².

Real-time quantitative reverse transcription-PCR

Total RNA was isolated from whole adipose tissue (n=7–8 per group) and liver (n=7 per group) using Tri reagent (Invitrogen, Carlsbad, CA) according to the manufacturer's protocol, and reverse transcribed to cDNA. Quantitative real time RT-PCR was performed using the Stratagene MX3000P instrument and the TaqMan Universal PCR Master Mix reagent kit, according to standard protocols. Primer and probe sequences for GAPDH, adiponectin, and F4/80 are as follows: GAPDH, forward primer, 5'AGCCTCGTCCCGTAGACAAA3'; reverse primer, 5'ACCAGGCGCCCAATACG3'; probe, HEX-5'AAATCCGTTACACCGACCTTACCA3'-BHQ1; adiponectin, forward primer, 5'GGAGAGAAAGGAGATGCAGGT3'; reverse primer, 5'CTTTCCTGCCAGGGGTTTC3'; probe, Cy5-5'AGGAGCTGAAGGGCCACGGG3'-BHQ2; F4/80, forward primer 5'GGAGGACTTCTCCAAGCCTATT3'; reverse primer 5'GGCCTCTCAGACTTCTGCTTT3'; probe Rox-5'ATACCTCCAGCAGCACATCCAG3'-BHQ2. SAA1/2 (hepatic isoforms); SAA3 (extra-hepatic isoform); SAA4 (constitutive isoform), MCP-1, TNF α primers and a FAM probe were obtained from Applied Biosystems (Assay-on-Demand). Assays were performed in triplicate and results are expressed as relative gene expression normalized to GAPDH mRNA levels.

Atherosclerosis quantification

The extent of atherosclerosis was measured using the *en face* technique as described previously¹⁹. Aortic root analysis on paraffin-embedded sections of the heart were analyzed for atherosclerotic lesion size, as described previously¹⁷.

Statistical analyses

Data are expressed as means \pm SD unless noted otherwise. Mean values were compared using ANOVA with Bonferroni post hoc testing for parametric data using GraphPad Prism program (Version 3.03, GraphPad Software, Inc., San Diego, CA). Data not normally distributed were analyzed using the Kruskal-Wallis test with Dunn's post test. p<0.05 was considered statistically significant. Multiple regression analysis was performed using the GraphPad InStat program (Version 3.05, GraphPad Software Inc., San Diego, CA).

RESULTS

Obesity, insulin resistance and hyperlipidemia are increased in LDLR^{-/-} mice fed a diabetogenic diet, and worsened in the presence of added cholesterol

LDLR^{-/-} mice fed a diabetogenic diet (DD) showed marked increases in weight over 24 weeks compared to chow fed controls (DD, 52.5±0.9g vs chow, 30±0.6g, p<0.01, Fig. 1A), as has been shown previously¹⁸. Addition of cholesterol to the diabetogenic diet (DDC) resulted in a similar weight gain (52.3±0.9g, p<0.01 vs chow), but was not significantly different compared to DD-fed animals. Fasting glucose was higher in the DD and DDC groups compared to chow-fed animals (p<0.001), but did not differ between the obese groups (Fig. 1B). Assessment of glucose homeostasis revealed that animals in both DD and DDC groups developed equal and significant glucose intolerance compared to chow diet fed controls (data not shown). Animals in both DD and DDC groups demonstrated hyperinsulinemia (Fig. 1C). However, plasma insulin levels were significantly higher in the DDC group (p<0.05), suggesting that these animals were the most insulin resistant. The calculated HOMA-IR index of the DD group was significantly higher than that of chow fed animals (p<0.001) (Fig 1D). The HOMA-IR value was highest in the DDC group (p<0.001 vs chow and p<0.05 vs DD), suggesting that this group was the most insulin resistant.

Hypertriglyceridemia and hypercholesterolemia developed in both groups of diabetogenic diet fed animals compared to chow-fed controls (Fig. 2A and B). Triglyceride levels were higher compared to chow-fed animals (p<0.001), but were not significantly different between the DD or DDC groups (Fig 2A). However, there was a small but statistically significant increase in plasma cholesterol in the DDC group compared to the DD-fed animals (p<0.05, Fig 2B). In addition, lipoprotein profiles of animals in the DDC group revealed lower HDL cholesterol and higher VLDL cholesterol levels compared to the DD group (Fig 2C).

Intra-abdominal adipose tissue characteristics are altered in LDLR^{-/-} mice by the addition of cholesterol to the diabetogenic diet

To determine changes in adipose tissue morphology and gene expression that occur with obesity and cholesterol feeding, epididymal (intra-abdominal) and inguinal (subcutaneous) adipose tissues harvested at the time of sacrifice were studied. Since macrophages in adipose tissue have been implicated in the pathogenesis of obesity-induced insulin resistance, we used immunohistochemistry to identify the presence of macrophages within adipose tissue. Staining with an antibody to macrophage Mac2 showed that the diabetogenic diets induced a significant increase in macrophages in epididymal adipose tissue (Fig. 3A&C). Areas stained for macrophages were significantly greater in the DDC tissue compared to chow-fed animals and the DD animals (p<0.001 and p<0.05 respectively, Figure 3C). Proteoglycan staining in this tissue was significantly increased in the DD and DDC groups (p<0.05 and p<0.01 vs chow, data not shown). Epididymal adipose tissue revealed similar adipocyte hypertrophy in both DD and DDC groups relative to controls (Fig. 3D). Adipocyte hypertrophy was also observed in the inguinal fat pads in DD and DDC groups (p<0.01, Fig 3E) but no evidence of macrophage infiltration or increased proteoglycan by immunostaining was noted in any of the groups (Fig. 3B). With real time RT-PCR, epididymal adipose tissue showed significantly decreased levels of adiponectin mRNA in both obese animal groups (Fig. 4A) compared to controls. mRNA levels of the macrophage marker F4/80 were increased in both DD and DDC groups (p<0.05 and p<0.001 respectively), with significantly higher levels in the DDC compared to the DD animals (p<0.05, Fig. 4B) confirming increased adipose tissue macrophages. mRNA levels of the marker for macrophage alternative activation, CD11c, were also significantly greater in the DDC (p,0.01 vs chow and p<0.05 vs DD; Supplemental data Figure I). There were no significant differences in inguinal fat adiponectin or F4/80 mRNA levels among the three groups (Fig. 4F&G).

Local inflammation is present in intra-abdominal adipose tissue in LDLR^{-/-} mice fed a diabetogenic diet without or with cholesterol

Cytokines secreted by adipose tissue macrophages can induce a local inflammatory response. Therefore we studied the extent of local adipose tissue inflammation by measuring expression of genes involved in inflammation by real time quantitative RT-PCR. Although TNF α mRNA levels were significantly increased in epididymal adipose tissue in both obese animal groups compared to controls ($p < 0.05$, Fig. 4C), levels were significantly higher in the DDC animals ($p < 0.05$). SAA3, the extrahepatic isoform of SAA produced by adipocytes and macrophages in mice, is a locally synthesized inflammatory molecule with chemoattractant properties^{23, 24}. SAA3 gene expression was significantly increased in the DDC group ($p < 0.05$, Fig. 4D) compared to DD. A similar pattern was also noted for the chemoattractant gene, MCP-1 (Fig. 4E). Inguinal adipose tissue showed no evidence of altered TNF α production (Fig 4H), but there was evidence of significantly elevated SAA3 in the DDC group (Fig. 4I), and of MCP-1 mRNA levels in both DD and DDC animals (Fig. 4J). Since expression levels of SAA3 suggested local inflammation in the adipose tissue depots, we performed immunohistochemical analysis for SAA within epididymal and inguinal fat depots (data not shown). In the epididymal fat pad, stained areas for SAA were 3-fold higher in the DD animals ($p < 0.05$) and 9-fold greater in the DDC group ($p < 0.01$) compared to chow-fed controls. SAA-stained areas were significantly higher in the DDC compared to DD group ($p < 0.05$). Inguinal adipose tissue did not show increased SAA staining, this being in contrast to SAA3 mRNA expression (Fig 4I). These findings could reflect rapid tissue degradation of SAA3, lack of translation of mRNA in inguinal adipose tissue, or lack of retention of SAA3 by proteoglycans, which were not detected in inguinal fat. Overall, however, these results suggest inflammatory changes occurring mainly at the level of the epididymal adipose tissue in these mice.

Chronic systemic inflammation, manifested as increased SAA levels in diabetogenic diet-fed animals, is worsened by the addition of dietary cholesterol

We assessed the presence of chronic systemic inflammation by measuring circulating SAA levels after 24 weeks on the diets. In mice, SAA functions as a key molecule that increases in inflammation²³. The circulating, inducible isoforms of SAA include SAA 1 and 2, are highly homologous and are derived from the liver. Measured SAA levels were significantly higher than controls ($1.4 \pm 0.6 \mu\text{g/mL}$) in the DD ($6.2 \pm 0.6 \mu\text{g/mL}$, $p < 0.05$) and DDC ($20.7 \pm 5.7 \mu\text{g/mL}$, $p < 0.001$) groups; in addition, SAA levels in the DDC group were significantly higher than in the DD-fed animals ($p < 0.05$, Fig. 5A). These levels, although elevated, are low compared to those attained during acute injury or inflammation²³, and suggest a state of chronic, inflammation in both groups of obese mice. Circulating SAA levels correlated with insulin levels ($r^2 = 0.43$, $p = 0.001$), suggesting that greater insulin resistance is associated with higher levels of SAA. Hepatic mRNA expression of SAA was also increased significantly in the DDC animals ($p < 0.001$ vs chow and $p < 0.01$ vs DD, Fig. 5B). Hepatic expression of the constitutive form of SAA i.e. SAA4, did not change in any of the groups (data not shown).

Under physiological conditions, SAA is predominantly associated with HDL²³. However, we have shown previously that SAA may be associated with other lipoprotein particles in LDLR^{-/-} mice fed high fat diets¹⁷. Therefore, we performed FPLC and analyzed fractions for the presence of SAA on other lipoproteins. In LDLR^{-/-} mice fed both diabetogenic diets, SAA was found on very low density/intermediate density lipoproteins (VLDL/IDL) and LDL in addition to HDL (Fig. 5C). The lipoprotein distribution suggested that mice fed DDC had more VLDL particles (Fig 5C, bottom panel), whereas the DD-fed animals had more LDL particles (Fig 5C, middle panel). The lipoprotein distribution of SAA was similar with both diabetogenic diets. However, since the DDC group had more non-HDL particles and higher SAA levels, they likely had more SAA in non-HDL particles than the DD animals.

Atherosclerosis is increased in the presence of diet-induced obesity, insulin resistance and elevated SAA levels, and worsened by dietary cholesterol

We next assessed atherosclerosis and found that mice fed the diabetogenic diets for 24 weeks had significantly increased atherosclerotic lesion area by *en face* analysis as compared to chow-fed controls ($p < 0.05$). There was a significant increase in atherosclerotic area in the DDC group compared to control ($p < 0.001$) and DD animals ($p < 0.05$, Fig. 6A). Similarly, maximal cross-sectional area of lesions in the aortic sinus was significantly greater in mice fed the DDC diet compared to either DD or chow fed groups (Fig. 6B). Immunohistochemistry of aortic root lesions showed significantly increased macrophage (Mac2 antibody stained) areas within lesions in the DDC group ($p < 0.001$ vs chow and $P < 0.05$ vs DD, Fig. 6C). This staining pattern is similar to that seen in the epididymal adipose tissue where the greatest Mac2 staining was noted in the DDC adipose tissue (Fig 3A&C). Staining with anti-SAA antibody revealed increased SAA immunostaining in the DDC group compared to chow ($p < 0.001$) and DD ($p < 0.05$) (Fig. 6D).

To further study the contribution of variables such as plasma cholesterol, insulin and SAA to atherosclerosis in these two groups of animals, we performed a multiple regression analysis. While cholesterol ($p = 0.36$) and insulin levels ($p = 0.074$) did not predict the development of atherosclerosis, $\log SAA$ ($p < 0.002$) was a predictor of atherosclerotic lesion areas in the obese animal groups, suggesting the slight increase in cholesterol levels noted in the DDC animals compared to the DD group did not play a major role in the increased atherosclerosis in this setting. Lipoproteins also did not contribute to atherosclerosis in this regression model.

DISCUSSION

Obesity is associated with increased insulin resistance^{25, 26}, and a predisposition to diabetes and cardiovascular disease in humans²⁷. Obesity also is associated with chronic, low-grade, systemic inflammation in both mice⁹ and humans²⁸. Our study confirmed that consumption of diabetogenic diets (high in both fat and carbohydrates) led to obesity, insulin resistance, low-grade inflammation, and accelerated atherosclerosis in LDLR^{-/-} mice.

We previously reported that the addition of a small amount of cholesterol to a Western-type diet was associated with chronic systemic inflammation, as evidenced by a modest increase in circulating levels of the inflammatory protein, SAA, and increased atherosclerosis¹⁷. Therefore, we questioned whether dietary cholesterol would further increase inflammation and atherosclerosis in an obese, insulin resistant mouse model. While addition of cholesterol to the diabetogenic diet increased systemic inflammation beyond that seen with the diabetogenic diet alone, we were surprised to find markedly increased inflammatory changes in adipose tissue. The addition of dietary cholesterol led to the accumulation of significantly more macrophages in epididymal adipose tissue, despite both obese groups gaining an equivalent amount of weight. Increased F4/80 mRNA provides additional evidence for macrophage accumulation, and increased TNF α and SAA3 mRNA suggests more local inflammation. Interestingly, the inflammatory changes were limited to epididymal (intra-abdominal) adipose tissue and were not observed in inguinal (subcutaneous) fat, despite increased inguinal fat mRNA levels of MCP-1 and SAA3, both known chemotactic factors^{24, 29}.

Inflammatory changes in epididymal adipose tissue were accompanied by insulin resistance, as evidenced by increased plasma insulin levels and HOMA-IR values, greatest in the group fed the diabetogenic diet with added cholesterol. This observation is consistent with the notion that adipose tissue inflammation contributes to insulin resistance⁸.

Local inflammation in epididymal adipose tissue in obese mice was accompanied by increased circulating levels of SAA, a marker of systemic inflammation, these changes being

significantly greater in mice fed the diabetogenic diet with added cholesterol. Whether these hepatic changes resulted from direct exposure of the liver to chylomicrons/chylomicron remnants with increased cholesterol content, to adipose tissue-derived cytokines, or both, is unknown. However, it seems likely that the hepatic inflammatory response is mediated by adipose-tissue derived inflammatory cytokines for at least two reasons. First, cytokines such as TNF α and interleukin-6 have been strongly implicated in the up-regulation of hepatic SAA synthesis³⁰. Second, the majority of hepatic blood flow derives from the portal circulation that drains intra-abdominal adipose depots. Moreover, no detectable inflammatory response was seen in subcutaneous adipose tissue, further implicating factors derived from intra-abdominal fat as the source of the hepatic inflammatory response.

Atherosclerosis was increased in both groups of obese mice, more so in animals that received added dietary cholesterol. Interestingly, macrophage staining in aortic sinus lesions also was greatest in the DDC group, similar to observations in epididymal adipose tissue. Multiple variable analysis of cholesterol, lipoproteins, insulin and SAA showed that only logSAA significantly predicted atherosclerosis in this model, similar to a recent observation in cholesterol-fed rabbits³¹. These findings suggest that low-grade inflammation, and specifically, an increase in SAA levels, might play a causal role in atherogenesis. Moreover, SAA immunostaining of aortic lesions also was greatest in the DDC group. As shown previously¹⁷, some SAA was present on lipoproteins other than HDL, the lipoprotein on which most SAA has been thought to be transported through plasma²³. All SAA isoforms have proteoglycan-binding domains²³, and we previously have suggested that the presence of SAA on lipoproteins (HDL and non-HDL) might facilitate their retention by vascular proteoglycans²¹. The presence of SAA on HDL could render these lipoproteins pro-atherogenic and SAA on VLDL or LDL might further increase the retention of these atherogenic lipoproteins, thereby increasing their ability to promote atherogenesis.

Our multivariate analysis also suggests that the increased atherosclerosis in the DDC group was not simply due to the slightly greater degree of hypercholesterolemia. However, there was a marked redistribution of lipoproteins in the DDC animals with greater VLDL cholesterol compared to the DD animals, which had greater LDL cholesterol. Therefore, the contribution of this altered lipoprotein distribution to the increased atherosclerosis in the DDC group cannot be eliminated.

Our findings are consistent with a “two-hit” hypothesis for the pathogenesis of inflammation and atherosclerosis in this mouse model. First, weight gain resulting from consumption of a “diabetogenic” diet leads to adipocyte expansion and macrophage accrual in adipose tissue, which appears to be depot-specific and limited to intra-abdominal adipose tissue. Macrophage accumulation in adipose tissue appears to be only in part related to the increased expression of the chemokines such as MCP-1^{29, 32} and extrahepatic SAA³²⁴, since macrophages were not observed in subcutaneous fat despite increased expression of these chemokines. The lack of detectable proteoglycan might explain the absence of SAA in subcutaneous adipose tissue, since our previous work suggests that proteoglycans may be necessary for SAA binding to tissue^{17, 21}. The second “hit” appears to be associated with the addition of cholesterol to the diabetogenic diet, although the mechanism by which dietary cholesterol leads to additional macrophage infiltration into intra-abdominal adipose tissue is unclear at this time. One possibility is that cholesterol, or perhaps oxysterols formed by oxidation of dietary cholesterol³³, are delivered to directly adipose tissue by chylomicrons or chylomicron remnants formed after lipolysis of chylomicron triglycerides by adipose tissue lipoprotein lipase. This could be a potential source of adipose cytotoxicity, which has been postulated as a cause of macrophage accumulation in adipose tissue³⁴.

Clinical implications of our study are particularly relevant to patients with familial hypercholesterolemia, a condition in which mutations in the LDL receptor cause significant hypercholesterolemia. In these patients, the accumulation of visceral fat has been shown to be associated with higher insulin levels and an increased cardiovascular risk³⁵, similar to findings in our mouse model.

In summary, the addition of dietary cholesterol to an obesity-inducing diabetogenic diet results in inflammatory changes beyond those seen with obesity alone. These changes appear to be due, at least in part, to increased accumulation of macrophages in adipose tissue and may have implications for the pathogenesis of insulin resistance, inflammation and atherosclerosis in obese human subjects.

Supplementary Material

Refer to Web version on PubMed Central for supplementary material.

ACKNOWLEDGEMENTS

This work was supported by an American Diabetes Association Mentor-based Postdoctoral Fellowship award (S.S), an American Heart Association Fellowship award (C.Y.H.), NIH grants HL030086, DK002456, DK035818.

REFERENCES

- Hotamisligil GS. Inflammation and metabolic disorders. *Nature* 2006;444:860–867. [PubMed: 17167474]
- Festa A, D'Agostino R Jr, Howard G, Mykkanen L, Tracy RP, Haffner SM. Chronic subclinical inflammation as part of the insulin resistance syndrome: the Insulin Resistance Atherosclerosis Study (IRAS). *Circulation* 2000;102:42–47. [PubMed: 10880413]
- Shoelson SE, Lee J, Goldfine AB. Inflammation and insulin resistance. *J Clin Invest* 2006;116:1793–1801. [PubMed: 16823477]
- Lemieux I, Pascot A, Prud'homme D, Almeras N, Bogaty P, Nadeau A, Bergeron J, Despres JP. Elevated C-reactive protein: another component of the atherothrombotic profile of abdominal obesity. *Arterioscler Thromb Vasc Biol* 2001;21:961–967. [PubMed: 11397704]
- Poitou C, Viguier N, Canello R, De Matteis R, Cinti S, Stich V, Coussieu C, Gauthier E, Courtine M, Zucker JD, Barsh GS, Saris W, Bruneval P, Basdevant A, Langin D, Clement K. Serum amyloid A: production by human white adipocyte and regulation by obesity and nutrition. *Diabetologia* 2005;48:519–528. [PubMed: 15729583]
- Weisberg SP, McCann D, Desai M, Rosenbaum M, Leibel RL, Ferrante AW Jr. Obesity is associated with macrophage accumulation in adipose tissue. *J Clin Invest* 2003;112:1796–1808. [PubMed: 14679176]
- Canello R, Henegar C, Viguier N, Taleb S, Poitou C, Rouault C, Coupaye M, Pelloux V, Hugol D, Bouillot JL, Bouloumie A, Barbatelli G, Cinti S, Svensson PA, Barsh GS, Zucker JD, Basdevant A, Langin D, Clement K. Reduction of macrophage infiltration and chemoattractant gene expression changes in white adipose tissue of morbidly obese subjects after surgery-induced weight loss. *Diabetes* 2005;54:2277–2286. [PubMed: 16046292]
- Berg AH, Scherer PE. Adipose tissue, inflammation, and cardiovascular disease. *Circ Res* 2005;96:939–949. [PubMed: 15890981]
- Xu H, Barnes GT, Yang Q, Tan G, Yang D, Chou CJ, Sole J, Nichols A, Ross JS, Tartaglia LA, Chen H. Chronic inflammation in fat plays a crucial role in the development of obesity-related insulin resistance. *J Clin Invest* 2003;112:1821–1830. [PubMed: 14679177]
- Szalai AJ. The biological functions of C-reactive protein. *Vascul Pharmacol* 2002;39:105–107. [PubMed: 12616974]
- Stamler J, Shekelle R. Dietary cholesterol and human coronary heart disease. The epidemiologic evidence. *Arch Pathol Lab Med* 1988;112:1032–1040. [PubMed: 3052353]

12. McNamara DJ. Dietary cholesterol and atherosclerosis. *Biochim Biophys Acta* 2000;1529:310–320. [PubMed: 11111098]
13. Reardon CA, Getz GS. Mouse models of atherosclerosis. *Curr Opin Lipidol* 2001;12:167–173. [PubMed: 11264988]
14. Watanabe Y. Serial inbreeding of rabbits with hereditary hyperlipidemia (WHHL-rabbit). *Atherosclerosis* 1980;36:261–268. [PubMed: 7406953]
15. Moghadasian MH, Frohlich JJ, McManus BM. Advances in experimental dyslipidemia and atherosclerosis. *Lab Invest* 2001;81:1173–1183. [PubMed: 11555665]
16. Shekelle RB, Stamler J. Dietary cholesterol and ischaemic heart disease. *Lancet* 1989;1:1177–1179. [PubMed: 2566743]
17. Lewis KE, Kirk EA, McDonald TO, Wang S, Wight TN, O'Brien KD, Chait A. Increase in serum amyloid A evoked by dietary cholesterol is associated with increased atherosclerosis in mice. *Circulation* 2004;110:540–545. [PubMed: 15277327]
18. Schreyer SA, Vick C, Lystig TC, Mystkowski P, LeBoeuf RC. LDL receptor but not apolipoprotein E deficiency increases diet-induced obesity and diabetes in mice. *Am J Physiol Endocrinol Metab* 2002;282:E207–E214. [PubMed: 11739102]
19. Schreyer SA, Lystig TC, Vick CM, LeBoeuf RC. Mice deficient in apolipoprotein E but not LDL receptors are resistant to accelerated atherosclerosis associated with obesity. *Atherosclerosis* 2003;171:49–55. [PubMed: 14642405]
20. Matthews DR, Hosker JP, Rudenski AS, Naylor BA, Treacher DF, Turner RC. Homeostasis model assessment: insulin resistance and beta-cell function from fasting plasma glucose and insulin concentrations in man. *Diabetologia* 1985;28:412–419. [PubMed: 3899825]
21. O'Brien KD, McDonald TO, Kunjathoor V, Eng K, Knopp EA, Lewis K, Lopez R, Kirk EA, Chait A, Wight TN, deBeer FC, LeBoeuf RC. Serum amyloid A and lipoprotein retention in murine models of atherosclerosis. *Arterioscler Thromb Vasc Biol* 2005;25:785–790. [PubMed: 15692094]
22. Chen HC, Farese RV Jr. Determination of adipocyte size by computer image analysis. *J Lipid Res* 2002;43:986–989. [PubMed: 12032175]
23. Uhlir CM, Whitehead AS. Serum amyloid A, the major vertebrate acute-phase reactant. *Eur J Biochem* 1999;265:501–523. [PubMed: 10504381]
24. Han CY, Subramanian S, Chan CK, Omer M, Chiba T, Wight TN, Chait A. Adipocyte-derived serum amyloid A3 and hyaluronan play a role in monocyte recruitment and adhesion. *Diabetes* 2007;56:2260–2273. [PubMed: 17563062]
25. Ferrannini E, Natali A, Bell P, Cavallo-Perin P, Lalic N, Mingrone G. Insulin resistance and hypersecretion in obesity. European Group for the Study of Insulin Resistance (EGIR). *J Clin Invest* 1997;100:1166–1173. [PubMed: 9303923]
26. Hotamisligil GS, Shargill NS, Spiegelman BM. Adipose expression of tumor necrosis factor- α : direct role in obesity-linked insulin resistance. *Science* 1993;259:87–91. [PubMed: 7678183]
27. Lakka HM, Lakka TA, Tuomilehto J, Salonen JT. Abdominal obesity is associated with increased risk of acute coronary events in men. *Eur Heart J* 2002;23:706–713. [PubMed: 11977996]
28. Tataranni PA, Ortega E. A burning question: does an adipokine-induced activation of the immune system mediate the effect of overnutrition on type 2 diabetes? *Diabetes* 2005;54:917–927. [PubMed: 15793228]
29. Weisberg SP, Hunter D, Huber R, Lemieux J, Slaymaker S, Vaddi K, Charo I, Leibel RL, Ferrante AW Jr. CCR2 modulates inflammatory and metabolic effects of high-fat feeding. *J Clin Invest* 2006;116:115–124. [PubMed: 16341265]
30. Thorn CF, Lu ZY, Whitehead AS. Regulation of the human acute phase serum amyloid A genes by tumour necrosis factor- α , interleukin-6 and glucocorticoids in hepatic and epithelial cell lines. *Scand J Immunol* 2004;59:152–158. [PubMed: 14871291]
31. Van Lenten BJ, Wagner AC, Navab M, Anantharamaiah GM, Hama S, Reddy ST, Fogelman AM. Lipoprotein inflammatory properties and serum amyloid A levels but not cholesterol levels predict lesion area in cholesterol-fed rabbits. *J Lipid Res*. 2007
32. Kanda H, Tateya S, Tamori Y, Kotani K, Hiasa K, Kitazawa R, Kitazawa S, Miyachi H, Maeda S, Egashira K, Kasuga M. MCP-1 contributes to macrophage infiltration into adipose tissue, insulin resistance, and hepatic steatosis in obesity. *J Clin Invest* 2006;116:1494–1505. [PubMed: 16691291]

33. Staprans I, Pan XM, Rapp JH, Feingold KR. The role of dietary oxidized cholesterol and oxidized fatty acids in the development of atherosclerosis. *Mol Nutr Food Res* 2005;49:1075–1082. [PubMed: 16270280]
34. Cinti S, Mitchell G, Barbatelli G, Murano I, Ceresi E, Faloia E, Wang S, Fortier M, Greenberg AS, Obin MS. Adipocyte death defines macrophage localization and function in adipose tissue of obese mice and humans. *J Lipid Res* 2005;46:2347–2355. [PubMed: 16150820]
35. Nakamura T, Kobayashi H, Yanagi K, Nakagawa T, Nishida M, Kihara S, Hiraoka H, Nozaki S, Funahashi T, Yamashita S, Kameda-Takemura K, Matsuzawa Y. Importance of intra-abdominal visceral fat accumulation to coronary atherosclerosis in heterozygous familial hypercholesterolaemia. *Int J Obes Relat Metab Disord* 1997;21:580–586. [PubMed: 9226489]

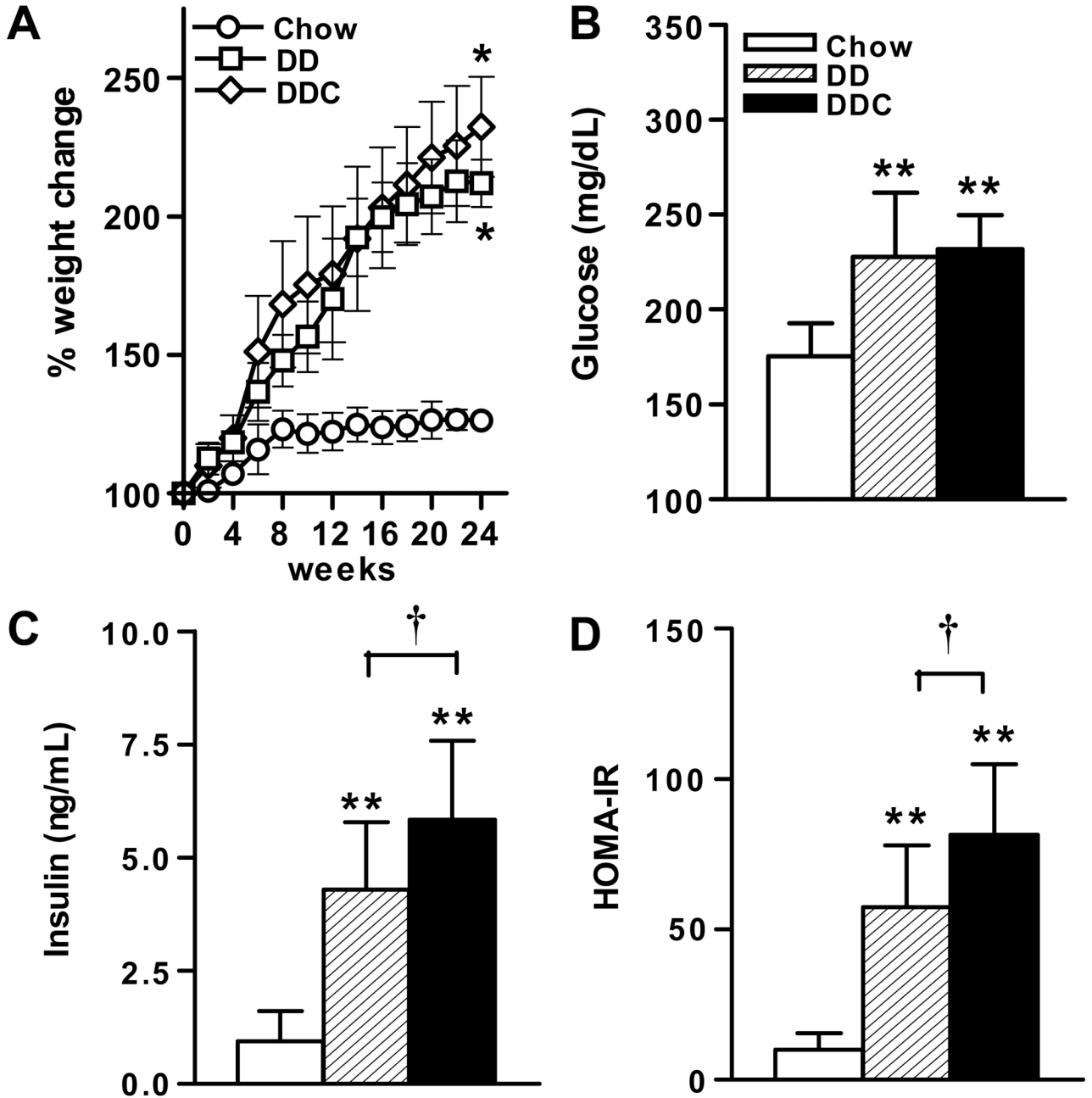


Figure 1. Metabolic effects of feeding LDLR^{-/-} mice diabetogenic diets without or with added cholesterol
 (A) Weight gain, (B) Fasting plasma glucose, (C) Plasma insulin, (D) HOMA-IR levels in mice fed chow (n=10, open bars), diabetogenic without (DD, n=15, hatched bars) or with added cholesterol (DDC, n=15, solid bars) diets for 24 weeks. *p<0.01, **p<0.001 vs chow, †p<0.05 vs DD. Values represent means±SD.

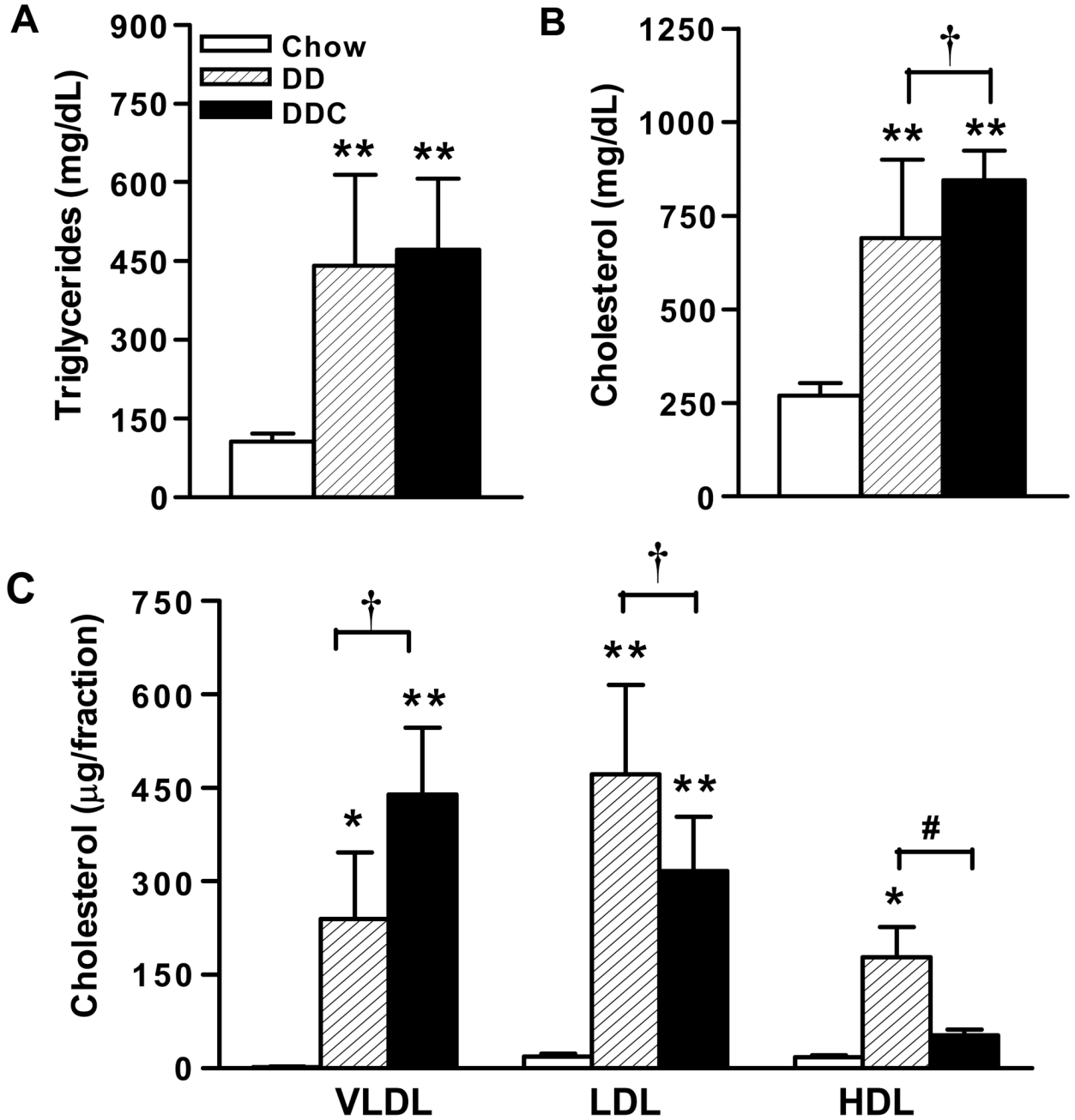


Figure 2. Effect of feeding diabetogenic diets in LDLR^{-/-} mice on lipids and lipoproteins
 (A) Plasma triglyceride, (B) Plasma cholesterol, (C) Lipoprotein distribution after 24 weeks of feeding diets. n=10 for chow, n=15 for DD and DDC groups. FPLC profiles shown in Figure 6. *p<0.05 vs chow, **p<0.001 vs chow, †p<0.05 vs DD, #p<0.01 vs DD. Values represent means±SD.

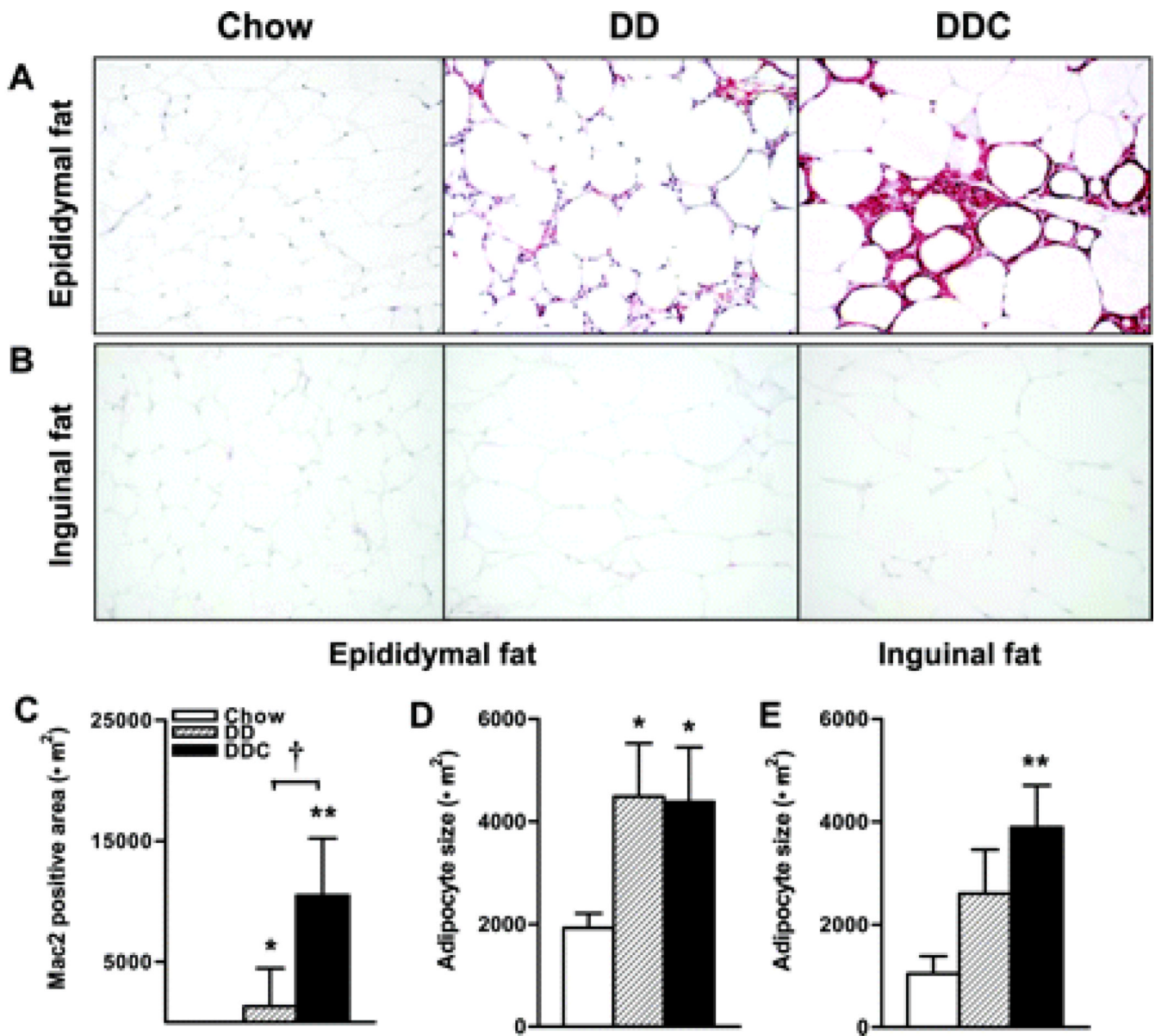


Figure 3. Adipose tissue macrophage accumulation is limited to intra-abdominal depots in obese LDLR^{-/-} mice fed diabetogenic diets and is increased by addition of dietary cholesterol (A) Epididymal adipose tissue stained with macrophage-specific antibody Mac2 (red), 200X magnification, n=8–10 per group. (B) Inguinal adipose tissue stained for Mac2. (C) Quantification of Mac2 staining. (D) Adipocyte size in epididymal adipose tissue. (E) Inguinal adipose tissue adipocyte size. *p<0.05 vs chow, **p<0.001 vs chow, †p<0.05 vs DD. AT, adipose tissue.

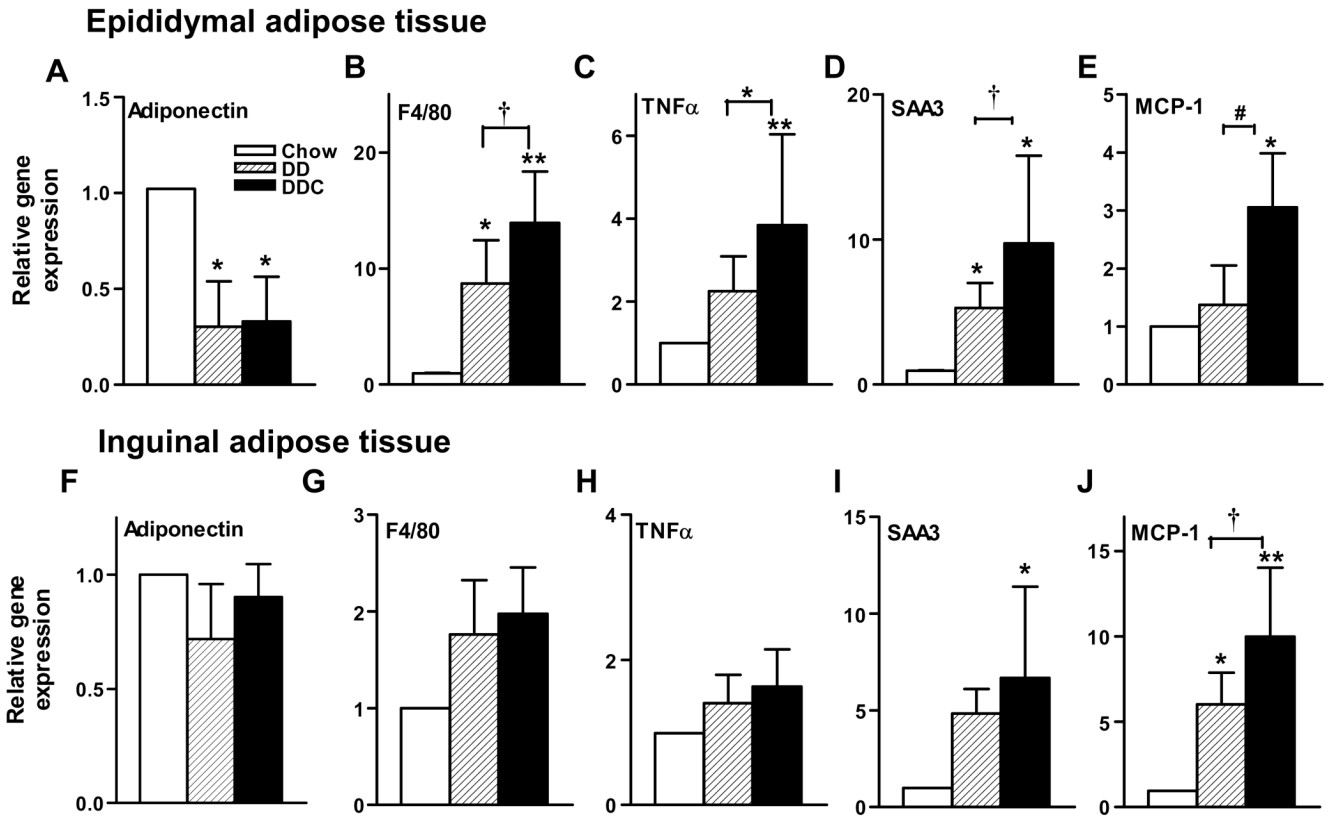


Figure 4. Differential expression of genes in epididymal and inguinal adipose tissue depots with addition of cholesterol to the diabetogenic diet

Top, epididymal adipose tissue expression of (A) adiponectin, (B) F4/80, (C) TNFα, (D) SAA3, (E) MCP-1 mRNA. Bottom, inguinal adipose tissue mRNA expression of (F) adiponectin, (G) F4/80, (H) TNFα, (I) SAA3, (J) MCP-1. Open bars, chow diet (n=7), hatched bars, DD (n=8) and solid bars, DDC (n=8). *p<0.05 vs chow; **p<0.01 vs chow; †p<0.05 vs DD, #p=0.01 vs DD. Values represent means±SD.

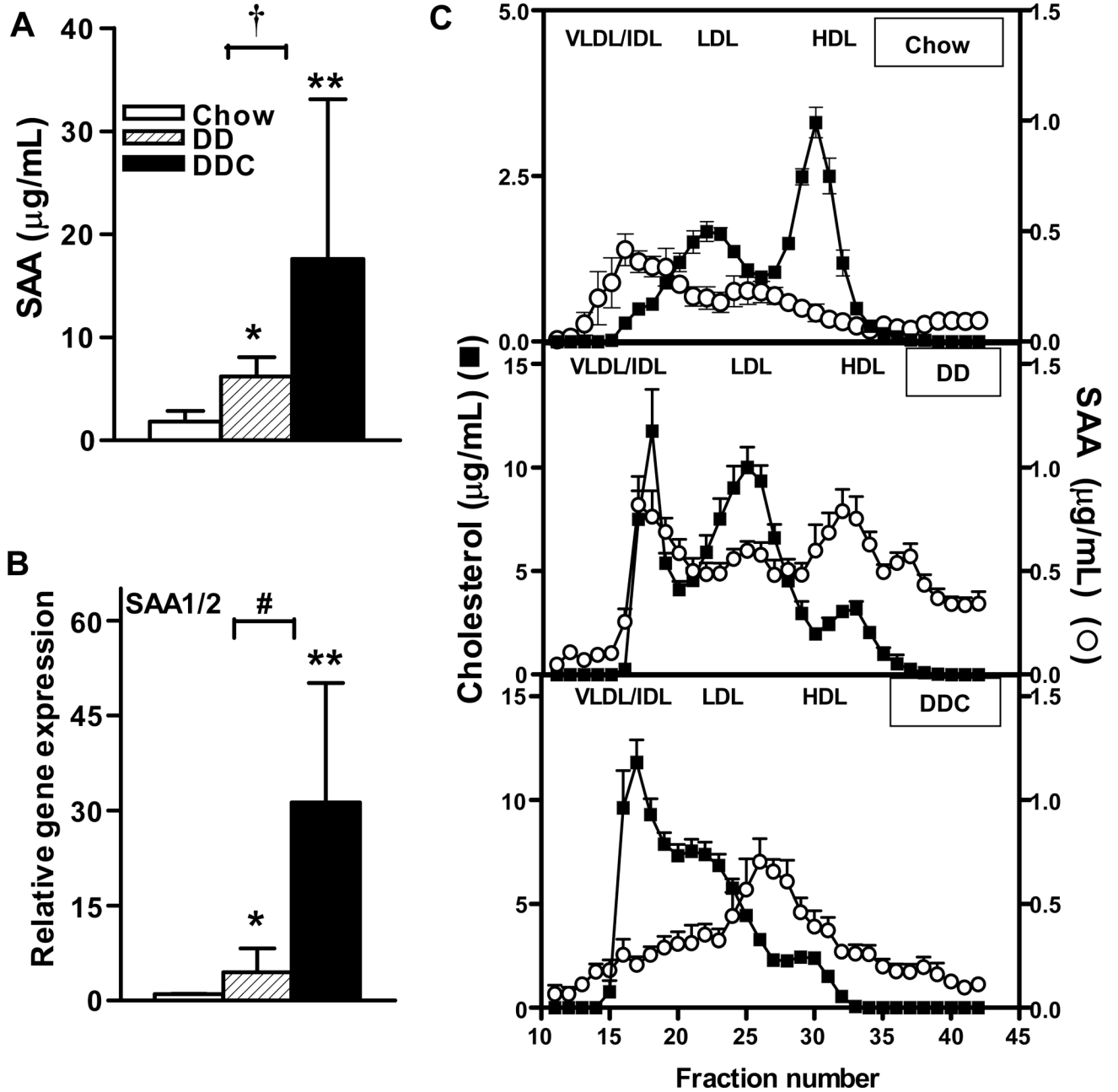


Figure 5. Circulating SAA levels are increased in LDLR^{-/-} mice fed the diabetogenic diet and further increased with the addition of dietary cholesterol
 (A) SAA levels (B) mRNA levels of hepatic isoforms SAA1/2, (C) Lipoprotein distribution of SAA and cholesterol in chow (top), DD (middle) or DDC (bottom) groups. n=3–6 animals/group. *p<0.05 vs chow, **p<0.001 vs chow, †p<0.05 vs chow and #p<0.01 vs DD. Values represent means±SD.

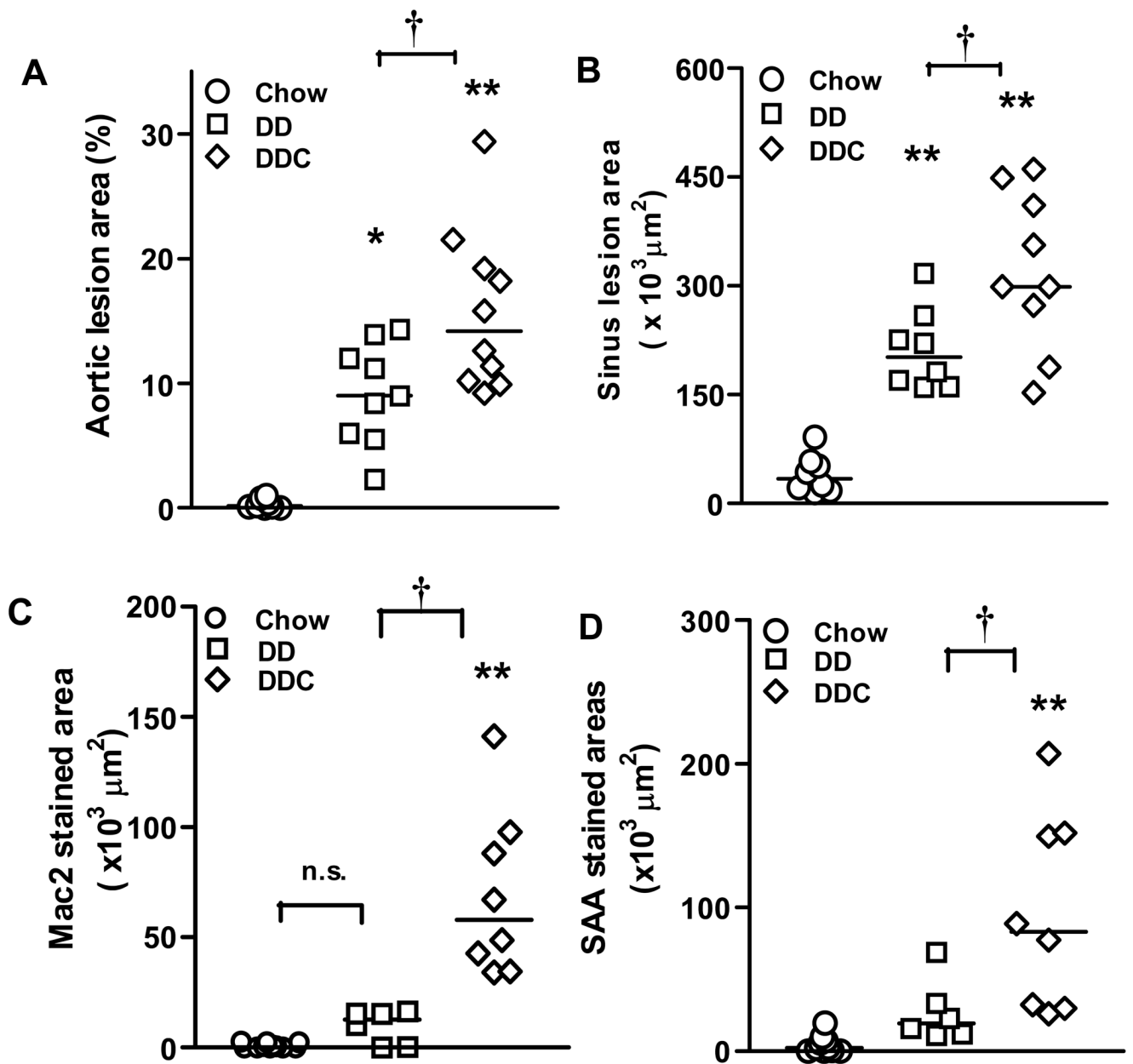


Figure 6. Aortic atherosclerosis is increased in obese, insulin resistant, chronically inflamed LDLR^{-/-} mice fed diabetogenic diets

(A) Aortic intimal and (B) sinus lesions. n=9–12 animals per group. (C) Mac2 staining of aortic sinus lesions. (D) Immunostaining of aortic sinus lesions for SAA. *p<0.01, **p<0.001 both vs chow, †p<0.05 vs DD.